

Effects of treatment protocols and subcutaneous implantation on bovine pericardium: a Raman spectroscopy study

Catherine P. Tarnowski

Shona Stewart

University of Michigan
Department of Chemistry
930 N. University Ave.
Ann Arbor, Michigan 48109-1055

Kelli Holder

Lori Campbell-Clark

R. J. Thoma

Alan K. Adams

Mark A. Moore

Sulzer Carbomedics Incorporated
Austin, Texas 78752

Michael D. Morris

University of Michigan
Department of Chemistry
930 N. University Ave.
Ann Arbor, Michigan 48109-1055
E-mail: mdmorris@umich.edu

Abstract. Using Raman microspectroscopy, we have studied mineral deposition on bovine pericardia, fixed according to three different protocols and either implanted subcutaneously or not implanted (controls). A lightly carbonated apatitic phosphate mineral, similar to that found in bone tissue, was deposited on the surface of a glutaraldehyde-fixed, implanted pericardium. Implanted pericardia fixed in glutaraldehyde followed by treatment in either an 80% ethanol or a 5% octanol/40% ethanol solution did not mineralize on implantation. Collagen secondary structure changes were observed on glutaraldehyde fixation by monitoring the center of gravity of the amide I envelope. It is proposed that the decrease in the amide I center of gravity frequency for the glutaraldehyde-fixed tissue compared to the nonfixed tissue is due to an increase in nonreducible collagen cross-links (1660 cm^{-1}) and a decrease in reducible cross-links (1690 cm^{-1}). The amide I center of gravity in the glutaraldehyde/ethanol-fixed pericardium was higher than the glutaraldehyde-fixed tissue center of gravity. This increase in center of gravity could possibly be due to a decrease in hydrogen bonding within the collagen fibrils following the ethanol pretreatment. In addition, we found a secondary structure change to the pericardial collagen after implantation: an increase in the frequency of the center of gravity of amide I is indicative of an increase in cross-links. © 2003 Society of Photo-Optical Instrumentation Engineers. [DOI: 10.1117/1.1559729]

Keywords: Raman; pericardium; fixation; glutaraldehyde; mineralization; ethanol.

Paper JBO 02014 received Mar. 6, 2002; revised manuscript received Sep. 16, 2002; accepted for publication Oct. 7, 2002.

1 Introduction

Use of animal tissues, typically porcine aortic valves or bovine pericardium, for replacement of defective or damaged heart valves in humans is an established surgical procedure. In preparation for heart valve replacement in humans, the tissues are typically fixed to maintain elasticity and mechanical properties once implanted *in vivo*.¹ Glutaraldehyde treatment is the most common method used to fix the replacement tissues.¹ Unfortunately, glutaraldehyde fixation also results in increased calcification of the tissues *in vivo*, leading to failure and the need for replacement.

The addition of glutaraldehyde to tissue creates cross-links by rapidly reacting with the amine groups of lysine and hydroxylysine amino acids in the collagen triple helix to form a relatively unstable Schiff base intermediate. Further reaction with other glutaraldehyde molecules results in a variety of cross-links, some of which contain glutaraldehyde polymers or pendant glutaraldehyde groups.² The presence of the extra glutaraldehyde groups, which can leach out either with time or with cross-link degradation, can result in increased cytotoxicity.^{1,3} Consequently, as the tissue encounters cells during implantation, it causes the cells to lyse, and their contents provide the precursors for mineral formation and deposition. Mineralization is also thought to occur because the

fixation also prevents the tissue from maintaining a low ionic calcium content.^{1,3}

Researchers have tried many fixation techniques to prevent tissue mineralization. Vyavahare and coworkers and Lee and colleagues have shown that fixation with glutaraldehyde followed by ethanol provides the implants with adequate elasticity as well as a resistance to calcification.^{4–6} Ethanol treatment removes lipids from the tissue while also decreasing the water content in the tissue on rehydration.⁵ Both of these effects have been suggested as mechanisms for the prevention of calcification by ethanol treatment, but the exact mechanisms that prevent mineralization are still not well understood.^{1,3,5,7,8}

Raman and Fourier-transform infrared (FTIR) spectroscopies are now extensively used to study mineralized tissues^{9–17} as well as soft tissues,^{4–6,18–24} because they provide information on mineral structure and changes in protein secondary structure. Raman spectroscopy is especially useful in the study of hydrated tissue specimens, because the relatively weak water spectrum does not obscure the rest of the spectrum. Raman spectroscopy is nondestructive and specimens can be used for other analyses after spectroscopic analysis.

The major protein component in pericardia is type 1 collagen.²⁵ Collagen has many bands in its Raman spectrum: the most prominent collagen bands are the amide stretches (amide III, C-N-H stretch, 1244 and 1270 cm^{-1} ; amide I, C-C-N stretch, 1662 cm^{-1}) and the CH_2 wag (1447 cm^{-1}).²⁶ Protein C-C backbone stretches are observed at 814 and 935 cm^{-1} , and the ring stretches of proline (918 cm^{-1}), hydroxyproline (853 and 873 cm^{-1}), and phenylalanine (1000 cm^{-1}) are also present.^{22,26,27} Changes in the collagen secondary structure are most notably manifested as changes in the amide I band contour (1650 to 1680 cm^{-1}). Wang, Galiotis, and Bader have shown that the amide I band shifts to higher frequencies when the collagen from a tendon is axially stretched.²³ Morris and colleagues have also demonstrated that stretched and damaged collagen exhibits high-frequency shoulders on the amide I band.²⁸ Lazarev, Grishkovsky, and Khromova have shown that the collagen band has an increased intensity ratio of the 1630/1660 cm^{-1} band frequencies with denaturation, and that with dehydration, the amide I components shift to higher frequencies.²⁹ Paschalis and colleagues, using FTIR spectroscopy, found that the amide I envelope for collagen with nonreducible and reducible cross-links contains vibrational bands near 1660 and 1690 cm^{-1} , respectively.¹⁷ In Raman spectroscopy, changes are also evident in the amide III band envelope (1240 to 1280 cm^{-1}), but are not as pronounced as those in the amide I region.

Raman spectroscopy is used to examine the effects of fixation and alcohol treatments on the bovine pericardium collagen secondary structure to better understand the mechanism for the prevention of mineralization and to identify the composition of the mineral deposited as a result of subcutaneous implantation.

2 Experimental

2.1 Specimen Preparation

Fresh bovine pericardia were obtained from an abattoir. Extraneous fat or muscle was removed and sections with heavy vasculature or attached ligaments were discarded. The fresh tissue was stored in chilled phosphate buffered saline (PBS, pH 7.4) until the time of treatment with HSHS (proprietary storage solution, Sulzer Carbomedics, Incorporated), glutaraldehyde, ethanol, or octanol.

2.1.1 HSHS storage (fresh tissues)

One group of bovine pericardium specimens was stored in HSHS until use. Prior to analysis or implantation, the tissue was placed in chilled PBS (pH 7.4) for a minimum of 24 hours. The HSHS-stored and PBS-rehydrated tissues served as controls for the other fixation techniques, because HSHS tissues behave as fresh, nonfixed tissues.

2.1.2 Glutaraldehyde fixation

Fresh bovine pericardia stored in PBS were transferred to a buffered solution of 0.25% glutaraldehyde for one week prior to analysis or implantation.

2.1.3 Ethanol and octanol/ethanol treatment

The ethanol- and octanol/ethanol-treated bovine pericardia were first fixed with glutaraldehyde as described before and

then transferred to either 80% ethanol buffered HEPES (10 mM) solution for three days prior to analysis or implantation, or to 5% octanol/40% ethanol buffered HEPES (10 mM) solution for three days prior to analysis or implantation.

2.2 Rat Subcutaneous Implantation

The rat subcutaneous model for assessment of tissue calcification has been described previously.²⁵ Briefly, 1.5- cm^2 samples of tissue were implanted subcutaneously in three-week-old Sprague-Dawley rats. After 60 days of implantation, the rats were euthanized and the tissue specimens withdrawn and immediately placed in formalin. Calcium and phosphorus levels in the tissues were determined by elemental analysis. Histological sections were prepared, stained with von Kossa's stain for phosphate, and evaluated for mineral content. Specimens were also subjected to differential scanning calorimetry and Raman spectroscopy studies.

2.3 Elemental Analysis

Retrieved implanted tissue specimens were digested in concentrated HCl and analyzed by inductively couple plasma/atomic emission spectroscopy. The group of implanted glutaraldehyde-fixed pericardia averaged 259.7 \pm 82.5 mg/g Ca, 130.3 \pm 39.9 mg/g P, and a von Kossa score of 2.5 (on a scale of 0 to 5), indicating extensive mineralization. The average for the glutaraldehyde/ethanol-fixed, implanted pericardia and the glutaraldehyde/octanol/ethanol-fixed, implanted pericardia were 3.7 \pm 1.2 mg/g and 30.5 \pm 69.6 mg/g Ca, respectively, 0.0 \pm 0.0 mg/g and 15.6 \pm 36.4 mg/g P, respectively, and von Kossa scores of 0.7 and 1.2 (no mineral detected). Specimens chosen for Raman spectroscopy were representative of the average for each respective group.

2.4 Differential Scanning Calorimetry

All tissues were hydrated in PBS for 24 hours prior to differential scanning calorimetry analyses. The fresh pericardium stored in the HSHS solution had a shrink temperature of 61.8°C. The glutaraldehyde-, glutaraldehyde/ethanol- and the glutaraldehyde/octanol/ethanol-fixed, nonimplanted tissues had shrink temperatures of 88.4, 87.4, and 86.4°C, respectively. All fixed tissues had higher shrink temperatures than the fresh tissue, indicative of an increased number of cross-links in the fixed tissues. The postglutaraldehyde treatments did not result in significant changes in the shrink temperature.

2.5 Raman Spectroscopy

Specimens representative of the various treatment production lots were chosen for Raman spectroscopic analysis. One specimen representative of each group was chosen for Raman spectroscopy. All specimens were placed in two consecutive 1-h immersions of PBS and then soaked in PBS overnight before spectroscopic analysis. Three nonimplanted specimens were examined: a fresh pericardium, a glutaraldehyde-fixed pericardium, and a glutaraldehyde/ethanol-fixed pericardium. Three implanted specimens were also examined: a glutaraldehyde-fixed pericardium, a glutaraldehyde/ethanol-fixed pericardium, and a glutaraldehyde/octanol/ethanol-fixed pericardium. Raman transects (lines of point spectra) were acquired on the smooth areas of the bovine pericardium. The instrument design has been described previously.³⁰ Briefly, a

785-nm diode laser (SDL, Incorporated, San Jose, California, 80 mW at specimen) was used as the excitation source. The laser light was focused to a 1.5- μm spot on the specimen using a 10 \times /0.50 NA objective (Zeiss, Fluar Series, Thornwood, New York) mounted on a BH-2 microscope frame (Olympus, Incorporated, Melville, New York). The Raman scatter was focused into a near infrared-optimized axial transmissive spectrograph (Kaiser Optical Systems, Incorporated, HoloSpec f/1.8i) fitted with a 25- μm slit (3 to 4 cm^{-1} spectral resolution) and dispersed onto either a liquid nitrogen-cooled, back-thinned charge-coupled device (CCD) camera (Roper Scientific, MASD, San Diego, California) or else a thermoelectrically cooled, back-thinned, deep-depletion camera (Andor Technology, Belfast, Ireland). A motorized motion stage (New England Affiliated Technologies, NEAT, Danaher Precision Systems, Salem, New Hampshire) moved the specimen at 5- μm increments under the laser spot to provide 10- μm spatial resolution. The transects ranged in length from 500 to 750 μm .

2.6 Data Analysis

Data were processed using MATLAB software (MathWorks, Incorporated, Natick, Massachusetts) via both vendor-provided and locally written scripts. Data were preprocessed by removing cosmic ray spikes (typically 1 or 2 per spectrum) and by subtracting the dark current. For factor analyses, the datasets were divided into two spectral subregions. The factor analysis consisted of a principal components analysis followed by manual rotation of only the nonnoise eigenvectors using nonnegativity and band shapes as constraints.^{31,32} The resulting linear combinations of the original eigenvectors are referred to as factors; each factor describes the spectral signature of a particular tissue component or a background component. Each factor has a corresponding score. The score describes the location and relative amount of that factor in the original dataset.

Center-of-gravity calculations were also used to examine the pericardial spectra. The advantage of using center-of-gravity measurements to examine changes in the amide I band is that they probe small changes in the overall band contour rather than just changes in the peak maximum. Prior to calculating the center of gravity of the amide I band, the amide I region was baselined using a quadratic baseline and then offset to zero. The center of gravity of the amide I envelope (1580 to 1700 cm^{-1}) was then calculated using Eq. (1):

$$\text{COG} = \frac{\sum I \times X}{\sum I}, \quad (1)$$

where I is the intensity at any wavenumber X within the amide I band envelope.^{28,33}

3 Results

3.1 Raman Spectra

The Raman spectra revealed the presence of an apatitic phosphate, similar to early deposited mineral in bone tissue,¹⁰ in the implanted glutaraldehyde-fixed pericardium [Fig. 1(b)]. The spectra from the rest of the implanted and nonimplanted pericardia contained only a collagen-dominated protein signature. A representative single-point spectrum from the nonimplanted glutaraldehyde-fixed specimen is shown in Fig. 1(a).

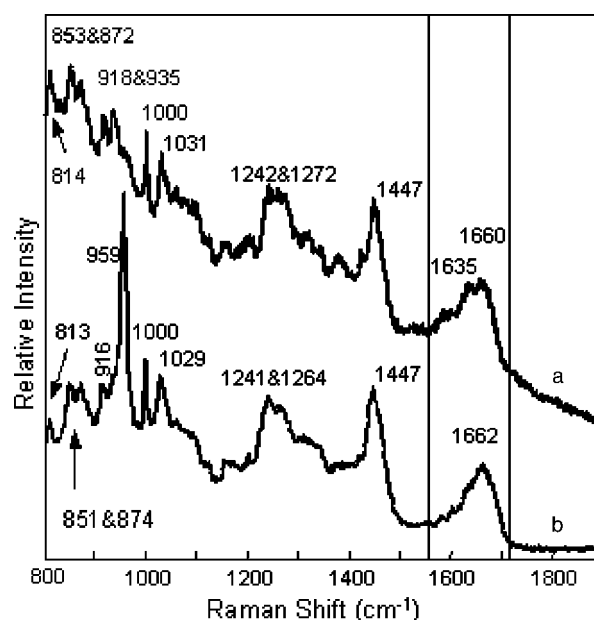


Fig. 1 Raw, single-point Raman spectra reveal the presence of an apatitic lattice in the glutaraldehyde-fixed, implanted specimen. (a) The glutaraldehyde-fixed, nonimplanted specimen has a collagen-dominated spectrum (C-C backbone stretches, 814 and 935 cm^{-1} ; hydroxyproline, 853 and 872 cm^{-1} ; proline, 918 cm^{-1} ; phenylalanine, 1000 cm^{-1} ; phosphate (nonapatitic), 1031 cm^{-1} ; amide III, 1242 and 1272 cm^{-1} ; CH_2 wag, 1447 cm^{-1} ; and amide I, 1635 and 1660 cm^{-1}). (b) The glutaraldehyde-fixed, implanted specimen has formed an apatitic phosphate (ν_1 , 959 cm^{-1}) on the collagen matrix [same assignments as for (a)]. Changes in the amide I envelope are highlighted in the boxed area. Spectra have been offset for clarity.

Comparison of the amide I regions of the glutaraldehyde-fixed, nonimplanted pericardium spectrum and the glutaraldehyde-fixed, implanted pericardium spectrum shows that there is a change in the collagen structure (Fig. 1, boxed area). The nonimplanted specimen spectrum has an amide I envelope with two readily visible bands at 1635 and 1660 cm^{-1} . However, in the implanted specimen, the ratio of the 1635 to the 1662 cm^{-1} intensity has decreased. A slight shoulder on the 1690 cm^{-1} side of the implanted specimen is also present. Similar results were seen in the spectra of tissues treated with the other fixation techniques.

3.2 Factor Analysis

3.2.1 Nonimplanted specimens

Individual factor analyses for the transects of the nonimplanted specimens showed the presence of only two factors for each of the specimens: a collagenous protein and a background factor. No factor containing any mineral spectral signatures was found.

3.2.2 Implanted specimens

The factor analysis of the glutaraldehyde-fixed and implanted specimen transect revealed the presence of four nonnoise factors: a carbonate-containing apatitic phosphate mineral factor [Fig. 2(b), $\text{PO}_4^{3-} \nu_1$ 959 cm^{-1} , $\text{PO}_4^{3-} \nu_3$ 1030 cm^{-1} , and $\text{CO}_3^{2-} \nu_1$ 1070 cm^{-1}], a collagenous protein signature [Fig. 2(a), amide III, 1242 cm^{-1} ; CH_2 wag, 1447 cm^{-1} ; and amide

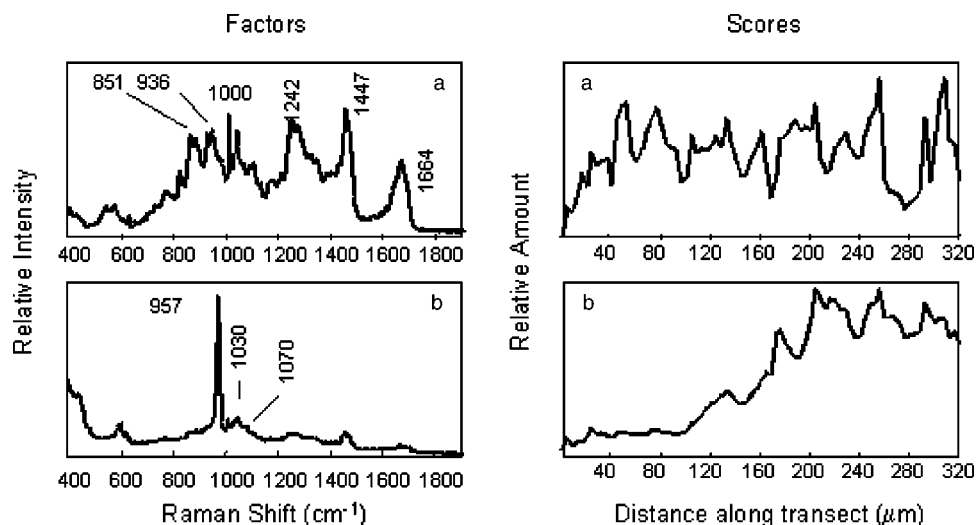


Fig. 2 Tissue factors and scores from the glutaraldehyde-fixed, implanted specimen reveal that mineral deposition was uneven over the surface of the pericardium. (a) The proteinaceous factor is mostly composed of collagen, while (b) the mineral factor contains bands from an apatitic phosphate lattice (ν_1 , 959 cm^{-1}) with a slight amount of carbonate (ν_1 , 1070 cm^{-1}). A score relates the amount of its corresponding factor at each point. Two nonnoise background factors were omitted for clarity.

I, 1664 cm^{-1}], and two background factors (not shown). The score, which describes the relative amount and location of a factor along the transect, shows that the relative amount of collagen was fairly even [Fig. 2, score (a)], but the mineral score shows an appreciable increase in mineral content after 160 μm along the transect [Fig. 2, score (b)]. While the mineral deposition was irregular along the transect, no evidence for chemical changes in the collagen or the mineral was found. Separate factor analyses of the glutaraldehyde/ethanol- and the glutaraldehyde/octanol/ethanol-fixed implanted specimen transects revealed the presence of three nonnoise factors for each of the specimens. The only nonbackground factor was a collagenous protein; no mineral was found.

3.3 Center-of-Gravity Calculations

Center-of-gravity calculations revealed that there was a slight difference in the contour of the amide I envelope of the nonimplanted pericardia. The fresh and the glutaraldehyde/ethanol-fixed specimens have similar center of gravities, while the glutaraldehyde-fixed pericardium tissue has a center of gravity at a lower frequency (Fig. 3). There was little difference in the amide I envelope center of gravity within the implanted pericardia; however, the implanted tissue and the nonimplanted have center of gravities that differ by about 10 cm^{-1} (Fig. 3).

4 Discussion

4.1 Mineralization

The glutaraldehyde-fixed specimen was the only fixed pericardium specimen that mineralized on implantation. A lightly carbonated apatitic mineral, similar to that found in bone tissue, was deposited unevenly on the surface of the pericardium. The uneven mineral deposition could be due to local irregularities in the tissue or changes in the collagen structure; further studies are needed to better elucidate the composition and structure of these mineral nucleation sites. Glutaraldehyde

fixation followed by either 80% ethanol or 40% ethanol/5% octanol treatment prevented mineralization during the 60 days of implantation. These results are consistent with the findings of previous studies that glutaraldehyde-fixed tissues will calcify once placed *in vivo*, while those cross-linked by glutaraldehyde and treated with ethanol mixtures (>50%) do not.⁴⁻⁶

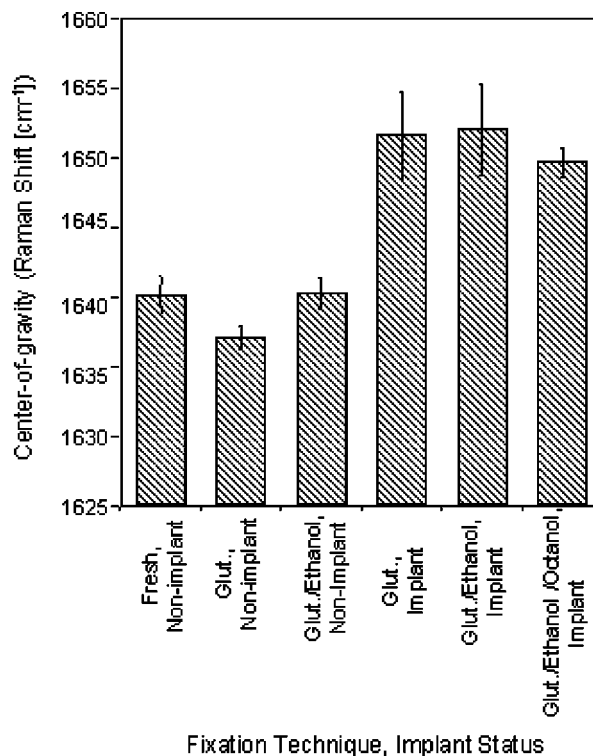


Fig. 3 Center-of-gravity measurements for the nonimplanted and implanted specimens. The amide I center-of-gravity measurements are higher for the implanted specimens than the nonimplanted specimens. The statistical uncertainties are equal to one standard deviation.

Interestingly, using FTIR spectroscopy, Vyavahare and co-workers demonstrated that there was significant calcification of porcine aortic valves after treatment with glutaraldehyde and 40% ethanol.⁴ In this work, the pericardium treated with a 40% ethanol/5% octanol mixture showed no evidence of calcification.

4.2 Amide I Center-of-Gravity Measurements

4.2.1 Nonimplanted specimens—frequency shifts due to fixation

The Raman spectra and center-of-gravity calculations showed there was a slight change in the collagen secondary structure as a result of the glutaraldehyde fixation (nonimplanted pericardia) compared to the nonimplanted fresh tissue and the nonimplanted glutaraldehyde/ethanol-fixed tissue. The center of gravity of the glutaraldehyde-fixed, nonimplanted tissue is at lower frequency ($1637.1 \pm 0.8 \text{ cm}^{-1}$) than that of the fresh and the glutaraldehyde/ethanol-fixed tissues (1640.1 ± 1.4 and $1640.3 \pm 1.1 \text{ cm}^{-1}$, respectively). Because the differential scanning calorimetry (DSC) data indicates an increase in cross-linking, it is unlikely that the source of the decreased center-of-gravity frequency is collagen denaturation (observed as a decrease in the 1660 cm^{-1} band and an increase in the 1630 cm^{-1} band²⁹). Therefore, the small decrease in the center-of-gravity frequency is probably due to a conversion of reducible to nonreducible cross-links found in the tissue, observed as an increase in the 1660 cm^{-1} component of the amide I band with a corresponding decrease in the reducible carbonyls found in the tissue (1690 cm^{-1}).¹⁷

However, nonimplanted glutaraldehyde/ethanol-fixed tissue has a higher frequency center of gravity than the nonimplanted glutaraldehyde-fixed tissue. A plausible cause for the shift in the center of gravity to higher frequencies is due to changes in hydrogen bonding. When the glutaraldehyde-fixation is followed by ethanol treatment, the cross-linked tissue is dehydrated. Lazarev, Grishkovsky, and Khromova have shown that dehydrated protein amide I components dramatically shift (20 to 30 cm^{-1}) to an increased frequency due to a loss of hydrogen bonding.²⁹ On rehydration, glutaraldehyde/ethanol-fixed tissue typically has slightly reduced water content than before ethanol treatment.⁵ Because there is a reduced water content and therefore less hydrogen bonding within the collagen fibrils, we expect to see a slight shift to higher frequencies for the amide I components. It has been proposed that water-ethanol interactions are partially responsible for the prevention of mineralization in the glutaraldehyde/ethanol-fixed tissues.⁴

4.2.2 Implanted specimens—frequency shifts due to implantation

Inspection of the Raman spectra and the center-of-gravity measurements also reveals that there is a collagen structural change in the pericardia after implantation. The center-of-gravity measurements indicate a shift to higher frequencies for the implanted specimens versus the nonimplanted controls. This band shift could be due to an increased number of cross-links, seen as bands in the 1660 and 1690 cm^{-1} regions¹⁷; however, we cannot rule out an increased amount of tension in the tissue, observed as an increase in the higher frequency shoulder intensity.^{23,28} An increase in the number of

cross-links could be caused by the fixation of the explanted tissues in formalin (a 10% formaldehyde solution), as formaldehyde is also capable of forming cross-links in collagen. The amide I center of gravity of a nonimplanted fresh tissue fixed in formalin showed a 5-cm^{-1} shift to higher frequency than nonfixed, nonimplanted fresh tissue. The frequency shift due to formalin fixation alone was not as large as what was seen in the implanted and formalin-fixed specimens (10 cm^{-1}), implying that the center-of-gravity frequency shifts between the nonimplanted and implanted tissues were due to both formalin fixation and protein secondary structure changes incurred on implantation. The protein secondary structure changes could be found either in the form of increased number of cross-links due to implantation or in the form of mechanical deformation due to implantation; we cannot identify the exact source of the increased center of gravity from this study.

5 Conclusions

Using Raman spectroscopy, we have identified the mineral formed on glutaraldehyde-fixed, implanted bovine pericardium as a lightly carbonated apatitic phosphate, similar to that found in bone tissue. We have demonstrated that glutaraldehyde-fixed tissues followed by treatment in either an 80% ethanol or 5% octanol/40% ethanol solutions do not calcify *in vivo*. We have also observed a change in the collagen secondary structure on fixation and implantation of bovine pericardia. Interestingly, the addition of octanol (5%) to the ethanol treatment (40%) has been shown to provide additional resistance to calcification, in contrast to previous studies⁴ that have shown that values treated with 40% ethanol alone do not resist calcification. It is possible that the octanol may better extract the lipids from the tissue, thereby inhibiting calcification. We have shown in this work that the prevention of mineralization in glutaraldehyde-fixed tissues is correlated with incomplete rehydration of the tissues and the extraction of lipids resulting from the ethanol and ethanol/octanol treatments, consistent with other studies of fixed porcine aortic valve tissues.^{4–6} It is possible that the ethanol and ethanol/octanol treatments may change the rate at which the glutaraldehyde groups incorporated into the collagen cross-links are released from the tissue, decreasing the cytotoxicity and therefore preventing mineralization. Further studies are needed to fully examine the effect of the ethanol and octanol treatments on the tissues.

Acknowledgments

M.A.M. and C.P.T. wish to thank the University of Michigan Bone Core Research Center through NIH grant AR P30 46024 for financial support.

References

1. F. J. Schoen and R. J. Levy, "Tissue heart valves: Current challenges and future research perspectives," *J. Biomed. Mater. Res.* **47**(4), 439–465 (1999).
2. L. H. H. Olde Damink, P. J. Dijkstra, M. J. A. Van Luyn, P. B. Van Wachem, P. Nieuwenhuis, and J. Feijen, "Glutaraldehyde as a crosslinking agent for collagen-based biomaterials," *J. Mater. Sci.: Mater. Med.* **6**(8), 460–472 (1995).
3. C. E. Schmidt and J. M. Baier, "Acellular vascular tissues: Natural biomaterials for tissue repair and tissue engineering," *Biomaterials* **21**, 2215–2231 (2000).

4. N. Vyavahare, D. Hirsch, E. Lerner, J. Z. Baskin, F. J. Schoen, R. Bianco, H. S. Kruth, R. Zand, and R. J. Levy, "Prevention of bioprosthetic heart valve calcification by ethanol preincubation: Efficacy and mechanisms," *Circulation* **95**(2), 479–488 (1997).
5. N. Vyavahare, D. Hirsch, E. Lerner, J. Z. Baskin, R. Zand, F. J. Schoen, and R. J. Levy, "Prevention of calcification of glutaraldehyde-crosslinked porcine aortic cusps by ethanol preincubation: Mechanistic studies of protein structure and water-biomaterial relationships," *J. Biomed. Mater. Res.* **40**, 577–585 (1998).
6. C. H. Lee, N. Vyavahare, R. Zand, H. Kruth, F. J. Schoen, R. Bianco, and R. J. Levy, "Inhibition of aortic wall calcification in bioprosthetic heart valves by ethanol pretreatment: Biochemical and biophysical mechanisms," *J. Biomed. Mater. Res.* **42**(1), 30–37 (1998).
7. J. M. Gross, "Calcification of bioprosthetic heart valves and its assessment," *J. Thorac. Cardiovasc. Surg.* **121**, 428–430 (2001).
8. L. L. Demer, "Lipid hypothesis of cardiovascular calcification (editorial)," *Circulation* **95**(2), 297–298 (1997).
9. A. Carden and M. D. Morris, "Application of vibrational spectroscopy to the study of mineralized tissues (review)," *J. Biomed. Opt.* **5**(3), 259–268 (2000).
10. C. P. Tarnowski, M. A. Ignelzi, Jr., and M. D. Morris, "Mineralization of developing mouse calvaria as revealed by Raman microspectroscopy," *J. Bone Miner. Res.* **17**(6), 1118–1126 (2002).
11. J. A. Timlin, A. Carden, M. D. Morris, R. M. Rajachar, and D. H. Kohn, "Raman spectroscopic imaging markers for fatigue-related microdamage in bovine bone," *Anal. Chem.* **72**(10), 2229–2236 (2000).
12. J. J. Freeman, B. Wopenka, M. J. Silva, and J. D. Pasteris, "Raman spectroscopic detection of changes in bioapatite in mouse femora as a function of age and *in vitro* fluoride treatment," *Calcif. Tissue Int.* **68**, 156–162 (2001).
13. C. J. de Grauw, J. D. de Bruijn, C. Otto, and J. Greve, "Investigation of bone and calcium phosphate coatings and crystallinity determination using Raman microspectroscopy," *Cells Mater.* **6**(1–3), 57–62 (1996).
14. L. M. Miller, V. Vairavamurthy, M. R. Chance, R. Mendelsohn, E. P. Paschalis, F. Betts, and A. L. Boskey, "In situ analysis of mineral content and crystallinity in bone using infrared micro-spectroscopy of the ν_4 PO_4^{3-} vibration," *Biochim. Biophys. Acta* **1527**, 11–19 (2001).
15. H. Ou-Yang, E. P. Paschalis, W. E. Mayo, A. L. Boskey, and R. Mendelsohn, "Infrared microscopic imaging of bone: Spatial distribution of CO_3^{2-} ," *J. Bone Miner. Res.* **16**(5), 893–900 (2001).
16. R. Mendelsohn, E. P. Paschalis, P. J. Sherman, and A. L. Boskey, "Microscopic imaging of pathological states and fracture healing of bone," *Appl. Spectrosc.* **54**(8), 1183–1191 (2000).
17. E. P. Paschalis, K. Verdelis, S. B. Doty, A. L. Boskey, R. Mendelsohn, and M. Yamauchi, "Spectroscopic characterization of collagen cross-links in bone," *J. Bone Miner. Res.* **16**(10), 1821–1828 (2001).
18. H. P. Buschman, E. T. Marploe, M. L. Wach, B. Bennett, T. C. Bakker Schut, H. A. Bruining, A. V. Brusckhe, A. van der Laarse, and G. J. Puppels, "In vivo determination of the molecular composition of artery wall by intravascular Raman spectroscopy," *Anal. Chem.* **72**(16), 3771–3775 (2000).
19. T. C. Bakker Schut, M. J. H. Witjes, H. J. C. M. Sterenborg, O. C. Speelman, J. L. N. Roodenburg, E. T. Marple, H. A. Bruining, and G. J. Puppels, "In vivo detection of dyplastic tissue by Raman spectroscopy," *Anal. Chem.* **72**(24), 6010–6018 (2000).
20. M. G. Shim, L.-M. Wong Kee Song, N. E. Marcion, and B. C. Wilson, "In vivo near-infrared Raman spectroscopy: Demonstration of feasibility during clinical gastrointestinal endoscopy," *Photochem. Photobiol.* **72**(1), 146–150 (2000).
21. U. Utzinger, D. L. Heintzelman, A. Mahadevan-Jansen, A. Malpica, M. Follen, and R. Richards-Kortum, "Near-infrared Raman spectroscopy for *in vivo* detection of cervical precancers," *Appl. Spectrosc.* **55**(8), 955–959 (2001).
22. J. J. Baraga, M. S. Feld, and R. P. Rava, "In situ optical histochemistry of human artery using near infrared Fourier transform Raman spectroscopy," *Proc. Natl. Acad. Sci. U.S.A.* **89**, 3473–3477 (1992).
23. Y.-N. Wang, C. Galiotis, and D. L. Bader, "Determination of molecular changes in soft tissues under strain using laser Raman microscopy," *J. Biomech.* **33**, 483–486 (2000).
24. M. Shen, P. S. Lajos, D. Farge, M. Daudon, S. M. Carpentier, L. Chen, B. Martinet, and A. F. Carpentier, "Infrared spectroscopy in the evaluation of the process of calcification of valvular bioprostheses," *Ann. Thorac. Surg.* **66**(6), S236–S239 (1998).
25. F. J. Schoen, J. W. Tsao, and R. J. Levy, "Calcification of bovine pericardium used in cardiac valve bioprostheses: Implications for the mechanisms of bioprosthetic tissue mineralization," *Am. J. Pathol.* **123**, 134–145 (1986).
26. B. G. Frushour and J. L. Koenig, "Raman scattering of collagen, gelatin, and elastin," *Biopolymers* **14**, 379–391 (1975).
27. P. Tarakeshwar and S. Manogaran, "Proline and hydroxyproline zwitterions—an ab initio study," *J. Mol. Struct.: THEOCHEM* **417**, 255–263 (1997).
28. M. D. Morris, A. Carden, R. M. Rajachar, and D. H. Kohn, "Bone microstructure deformation observed by Raman microscopy," *Proc. SPIE* **4254**, 81–89 (2001).
29. Y. A. Lazarev, B. A. Grishkovsky, and T. B. Khromova, "Amide I band of IR spectrum and structure of collagen and related polypeptides," *Biopolymers* **24**, 1449–1478 (1985).
30. J. A. Timlin, A. Carden, M. D. Morris, J. F. Bonadio, C. E. Hoffler, K. M. Kozloff, and S. A. Goldstein, "Spatial distribution of phosphate species in mature and newly generated mammalian bone by hyper-spectral Raman imaging," *J. Biomed. Opt.* **4**(1), 28–34 (1999).
31. J. M. Shaver, K. A. Christensen, J. A. Pezzuti, and M. D. Morris, "Structure of dihydrogen phosphate ion aggregates by Raman-monitored serial dilution," *Appl. Spectrosc.* **52**(2), 259–264 (1998).
32. N. L. Jestel, J. M. Shaver, and M. D. Morris, "Hyperspectral Raman line imaging on an aluminosilicate glass," *Appl. Spectrosc.* **52**(1), 64–69 (1998).
33. W.-Y. Yeh and R. J. Young, "Deformation processes in poly(ethylene terephthalate) fibers," *J. Macromol. Sci., Phys.* **B37**, 83–118 (1998).